crystals

MDPI

Article

Defect Related Emission in Calcium Hydroxide: The Controversial Band at 780 cm^{-1}

Francesca Assunta Pisu, Daniele Chiriu *, Pier Carlo Ricci and Carlo Maria Carbonaro

Department of Physics, University of Cagliari, Cittadella Universitaria, 09042 Monserrato (CA), Italy; francescaassunta.pisu@dsf.unica.it (F.A.P.); carlo.ricci@dsf.unica.it (P.C.R.); cm.carbonaro@dsf.unica.it (C.M.C.)
* Correspondence: daniele.chiriu@dsf.unica.it; Tel.: +39-0706754827

Received: 17 February 2020; Accepted: 27 March 2020; Published: 1 April 2020

Abstract: Calcium hydroxide, a crystal involved in the cycle of calcination and carbonation of calcium oxide, finds several applications from cultural heritage to the dentistry branch or to the construction industry. When excited at 1064 nm, Raman spectra of calcium hydroxide show a broad composite band peaked at about 780 cm^{-1}, corresponding to 1170 nm. Since it is not observed with visible excitation, the origin of this band is debated, being assigned to some pre-existent luminescent impurities or some structural defect of the lime formed after the synthesis of the material. To shed light on the formation of this band, we synthetised the lime paste starting from pure calcite powders. The obtained fresh $Ca(OH)_2$ samples did not show any band in the investigated range, irrespective of the laser excitation applied. A detailed analysis of the excitation and emission spectra in the near infrared region did not show the 1170 nm band, supporting the hypothesis of a post-synthesis origin. Thus, we carried out thermal treatments at different temperatures (90–500 °C) and under different environments (in air or under nitrogen flux) on synthesised fresh $Ca(OH)_2$ powders. We also investigated the time evolution of the samples, monitoring the Raman spectra over 90 days after a specific treatment. The collected data support the hypothesis of a defect-related luminescence centre, whose formation depends on the temperature and environment of the treatment, which appears as a preferential site for the carbonation process of the calcium hydroxide. These results can be useful in the field of Cultural Heritage for dating purposes, and to determine the conservation state of $Ca(OH)_2$ containing relics to prevent the possible activation of degradation processes.

Keywords: portlandite; calcium oxide/hydroxide; Raman

1. Introduction

Among the natural oxide minerals (oxides, hydroxides, and oxyhydroxides) the metal oxides find large applications for their optical, electronic, and magnetic properties. They are widely characterised as solid catalysts and exploited for various reactions, including acid–base and redox reactions, oxidation, dehydration, dehydrogenation, and isomerisation [1,2]. Calcium oxide (CaO), known also as "burnt lime" or "quicklime", crystallises in the cubic space group Fm-3m. It is white, caustic, and alkaline at room temperature and can be easily prepared by thermal heating of calcium carbonate ($CaCO_3$). However, CaO is very unstable after cooling, and it spontaneously reacts with environmental CO_2, converting back to calcium carbonate or, in the presence of water, to calcium hydroxide ($Ca(OH)_2$). $CaCO_3$, commonly extracted for industrial purposes, appears as fine white powder, and it is widely retrieved in sedimentary rocks in the polymorph minerals calcite, trigonal space group R-3c, and aragonite, orthorhombic space group Pmcn. Calcium hydroxide ($Ca(OH)_2$, known as hydrated or caustic lime) is an inorganic compound obtained by mixing or slaking water with calcium oxide. It is a colourless crystal called Portlandite, typically found as white powder, belonging to the P3m1 space group.

Calcium oxide, calcium hydroxide, and calcium carbonate are the main protagonists of the carbonation/calcination cycle. Starting from calcite, it is possible to obtain calcium oxide via thermal treatment above 900 °C [3–6]. Calcium oxide can react with water or with carbon dioxide to form calcium hydroxide or, directly, calcium carbonate. As an alternative, calcium hydroxide reacts with CO_2, leading to calcium carbonate as the final product.

The calcium carbonate cycle can be summarised as follows:

$$CaCO_3 + heat \rightarrow CaO + CO_2 \quad (1)$$

$$CaO + H_2O \rightarrow Ca(OH)_2 \quad (2)$$

$$Ca(OH)_2 + CO_2 \rightarrow CaCO_3 + H_2O \quad (3)$$

All the calcium products obtained during the carbonation/calcination cycle are used in the construction industry as malt or plaster compound [7–10], indicated by the general term "lime". Indeed, the term "lime" is frequently used in this branch to indicate calcium-containing inorganic materials, in which carbonates, oxides, and hydroxides predominate. These products are exploited in the building industry to prepare the mortar, a paste obtained by adding the required quantity of water to a mixture of binding materials like cement or lime (mainly $CaCO_3$ or $Ca(OH)_2$) and fine aggregates like sand. According to the typology of binding material, the mortars are classified into lime mortar, gypsum mortar, or cement mortar. Lime plaster is a type of plaster composed of sand, water, and lime, usually calcium hydroxide.

In the present work, we are mainly concerned with the structural and optical properties of calcium hydroxide, one of the products of the calcium oxide cycle, as explained before, whose proprieties allow its exploitation in different technological fields, from industrial building (vide supra) to endodontics, from food and pharmaceutical industries to cosmetics and cultural heritage. As an example, $Ca(OH)_2$ was introduced into the endodontic field as a pulp-capping agent since the last century because of its antimicrobial activity against common endodontic pathogens [11–13]. In the cultural heritage field, its applications date back to several centuries ago, being used as a ligand and a white pigment. In the book "II Libro dell'Arte", Cennini called the calcium-carbonated phase mixed with calcium oxide/hydroxide by the name "Bianco di San Giovanni" [14]. It was identified in walls and panel paintings of the Middle Age, in Gothic mural paintings made during the 15th century [15], and it was also found mixed in the casein and egg tempera media in many wall paintings of Giotto [14]. Calcium oxide/hydroxide is used also in the "a fresco" technique as a binder, where the pigment mixed with water is applied to wet lime plaster.

Prompted by our interest in the analysis and conservation of art relics, in this study we deal with the attribution of a specific optical feature typically recorded in the vibrational spectra of calcium hydroxide. It is indeed worth mentioning that Raman spectroscopy is very suitable in the cultural heritage field because it is completely non-destructive and does not require any pre-treatment of the samples. Moreover, thanks to advances in technology devices in recent years, it is possible to collect excellent experimental data directly in situ, by means of optical fibers-coupled devices with a small and compact dispersive apparatus, keeping the relic and its conservation condition under control [16–20]. As for the calcium hydroxide, under 1064 nm laser excitation the Raman spectra of $Ca(OH)_2$-containing artifacts [5,21], such as paintings, antique texts [16], or mortars of ancient buildings made by grinding calcite stone (as reported by Vitruvio in his book "De architectura") showed a large composite band peaked at about 780 cm^{-1}, whose attribution is still debated, mainly because of the excitation dependence. The behaviour of this band appears correlated to the carbonation process, since its intensity presents a progressive decreasing as the time increases, whilst at the same time the formation of the typical band at 1087 cm^{-1} of calcium carbonate is observed [6]. This particular trend can be clearly associated to the reaction of slaked lime to the environmental atmosphere. For this reason, the mentioned band elicited our attention as a specific marker for those processes in which a reaction driven by environmental conditions takes place. That is the case of frescoes or

paintings and in general Cultural Heritage $Ca(OH)_2$-containing relics where a possible degradation should be monitored. Schmida and Dariz [22] studied the Raman and luminescence spectra of CaO, $Ca(OH)_2$, and $CaCO_3$ with three different excitation wavelengths (514.5 nm, 632.8 nm, and 784.8 nm) and excluded the vibrational nature of this band, hypothesizing a luminescence effect derived by impurity (rare earth) elements. On the same grounds, other authors [23] investigated the fluorescence of some calcium minerals, correlating the above mentioned band to rare earth impurities associated with a particular structure or phase of this compound. Chaix-Pluchery et al. [22,24] studied the Raman spectrum of calcium hydroxide (λ_{exc} = 514 nm) at different temperatures and identified the formation of a luminescence band around 1650 cm^{-1} (that is, 562 nm) [24], but no evidence could be found in their spectra of the 780 cm^{-1} band. The possibility that this band derives from the luminescence of unreacted CaO or from a carbonation product ($CaCO_3$) was also considered. Actually, the luminescence properties of CaO are well known, and they show a luminescence band out of the above-mentioned luminescence range recorded for hydroxide [25]. On the other hand, a study of calcite luminescence [26] suggests that the emission recorded in the UV range, much more energetic than the one observed in calcium hydroxide, could be related, once again, to the presence of Mn^{2+}, Ce^{3+}, or Eu^{3+} ion impurities [27].

From the reported results, it is clear that the possible presence of impurities in the compounds involved in the calcination cycle could be the origin of the emissions recorded in the near infrared (NIR) range under 1064 nm laser excitation. Another possibility is the formation of some kind of defects during the carbonation/calcination cycle itself. Indeed, depending on the environmental conditions (humidity and temperature), the cycle could re-start and proceed. Dubina et al. [28] reported that the lime conversion to calcium hydroxide and its subsequent carbonation strongly depends on the relative humidity (RH) at which the samples are held for 24 h in moist air at 80 °C. Below 20% RH, the lime converts to portlandite without carbonation, while for a higher RH concentration the partial carbonation becomes relevant. However, the conversion process and its connection, if any, to the origin of the mentioned bands, is not ascertained.

In order to discriminate the origin of this band, assigning it to a definite luminescent or vibrational conclusive feature, we characterised the lime paste by analysing Raman spectra excited with visible and NIR excitations and carrying out different thermal treatments of the samples, also under different environment conditions, to support the assessment of a luminescence defect related to the carbonation/calcination cycle. A complete understanding of the nature of this band can be useful in the field of Cultural Heritage for dating purposes, as well as to determine the conservation state of mural relics to prevent the possible activation of degradation processes.

2. Materials and Methods

2.1. Sample Preparation

Materials and $CaCO_3$ powder were obtained by crushing pure commercial calcite stone (Sigma Aldrich, 99.95% Suprapur). The samples were calcinated at 1000 °C for two hours in order to obtain CaO powder. The product was then wetted with distilled water and mixed to complete the reaction. Finally, the obtained $Ca(OH)_2$ was heated at different temperatures (90–200–300–400–500 °C) for 1 h to allow the formation of the 780 cm^{-1} band. The thermal treatment at 300 °C was carried out both in air and in nitrogen atmosphere.

The reported thermal treatments were carried out to achieve the same effect as the time decantation usually performed on slaked lime for several months (at least six months or more) in wide tanks in order to have a complete reaction of slaked calcium oxide with water and a complete oxygen substitution.

2.2. Experimental Set-Up

2.2.1. Raman Measurements

NIR micro Raman scattering measurements were carried out in backscattering geometry with the 1064 nm line of an Nd:YAG laser. Measurements were performed in the air at room temperature with a compact spectrometer (B&WTEK, Newark, NJ, USA) i-Raman Ex integrated system with a spectral resolution, as declared by the constructor, of less than 8 cm^{-1}. The spectra were collected with different acquisition times between 20 s and 80 s and power excitations between 20 and 40 mW concentrated in a spot of 0.3 mm^2 on the surface through the BAC151B Raman Video Micro-Sampling System equipped with a 20 × Olympus objective to select the area on the samples.

Visible micro Raman scattering measurements were obtained in backscattering geometry through the 532 nm line by a wavelength stabilised diode module (LASOS DPSS series) coupled with a Reflecting Bragg Grating (Optigrate-Braggrade 405) to narrow the laser line. Measurements were performed in the air at room temperature with a triple spectrometer Jobin-Yvonne Dilor integrated system with a spectral resolution of about 1 cm^{-1}. Spectra were recorded in the Stokes region by a 1200 grooves/mm grating monochromator and a charge-coupled device (CCD) detector system.

2.2.2. Photoluminescence (PL) and Photoluminescence Excitation (PLE) Measurements

Samples were excited with different laser sources at 405 nm, 532 nm, and 632.8 nm to collect the luminescence through a detection system composed by the spectrometer B&WTEK (Newark, USA) with a spectral 1040–1460 nm IR range (corresponding to a 100–2500 cm^{-1} Raman shift). The emission signal was collected in front face mode by a wide spectral range optical fiber of 200 μm diameter. In addition, we performed PLE measurements by selecting the light of a laser driven Xenon lamp (EQ-99X) with a set of filters of 10 nm bandwidth and collecting the emission signal by means of the previous detection system. All the emission spectra were recorded in the air at room temperature, and proper longpass filters (in wavelength) were applied when needed to remove the residual scattered excitation signal.

Finally, the modifications of the spectra were monitored for a period of 90 days to check the aging effect on the calcium hydroxide samples under standard environmental conditions (average temperature 20 °C, average pressure 1 atm, and 60% of average RH). This time period was estimated to be enough to evaluate the kinetic of the studied processes.

3. Results and Discussion

The target of our investigation is to assess the origin of the excitation-dependent band in the range of 700–800 cm^{-1}, observed in calcium hydroxide only under 1064 nm laser excitation. The discussion of the results is carried out by a comparison to the features at low and high wavenumbers (*vide infra*). The starting point is the vibrational spectrum of unheated fresh $Ca(OH)_2$ samples under different wavelength excitations (532 nm, 632.8 nm, and 1064 nm). In Figure 1, we compare a reference spectrum excited at 532 nm [29] to the spectra of our synthesised samples excited at 532 nm (Figure 1a) and 1054 nm (samples not subjected to thermal treatments–Figure 1b). The reference spectrum displays two narrow bands at about 252 and 357 cm^{-1} and a large composite band peaked at about 680 cm^{-1}, already assigned to the vibrations of the OH^- against the cations (two translational and one rotational E_g and A_{1g} modes) [30]. As reported in the figure, the spectra of our samples excited both in the visible and NIR range report the same vibration bands (the same result also holds for the 632.8 nm, not reported here for the sake of brevity). The spectrum excited at 1064 nm evidences a large band peaked at about 936 cm^{-1}, previously ascribed to the O–H out-of-plane bending mode of unbound water [31,32]. The reported spectra do not show any contribution in the 700800 cm^{-1} range irrespective of the laser excitation exploited, in contrast to the literature spectra of aged calcium hydroxide gathered under 1064 nm excitation.

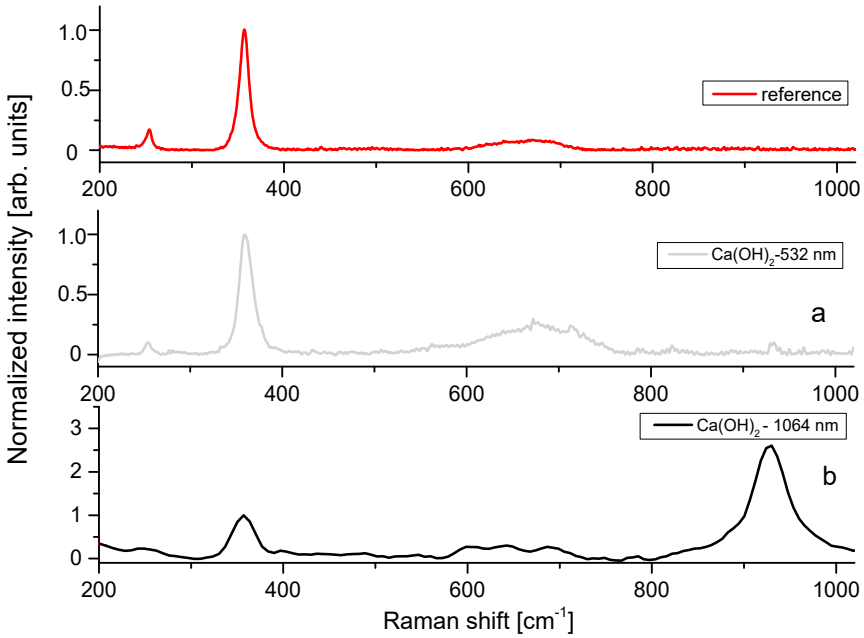

Figure 1. Raman spectrum of the lime paste: reference obtained with 532 nm excitation and the experimental sample, without thermal treatment, and with excitation at (**a**) 532 nm and (**b**) 1064 nm.

To support these results, we analysed the PLE measurements by monitoring the IR emission range, with no evidence, also in these experiments, of any contribution around 1170 nm (corresponding to the 780 cm^{-1} Raman band under 1064 nm laser excitation). These observations support the idea that the Raman band in the 700–800 cm^{-1} range reported in some literature spectra [22] does not belong to vibrational features nor to luminescence characteristics of fresh pure calcium hydroxide.

To further analyse the origin of these optical findings, we considered the carbonation/calcination cycle reported in the introduction. As already observed, the Raman spectrum excited with 1064 nm excitation (Figure 1b) shows a large contribution of the band at 936 cm^{-1}, associated with the O–H out-of-plane bending mode of unbound water, suggesting a large content of water in our samples not reported in the literature spectra of aged lime. Indeed, the reported spectra were collected on the raw samples, not subjected to any heat treatment. To reduce the water content and speed up the drying process of the synthetised $Ca(OH)_2$, we heated the samples at different temperatures in the 90–500 °C range. We measured the Raman spectra of the heated samples by exciting, once again, the vibration modes with visible and NIR laser sources (532, 632.8, and 1064 nm). Whilst no contributions were detected in the 700–800 cm^{-1} range with visible excitations, a large temperature-dependent band peaked at about 780 cm^{-1} is recorded when exciting at 1064 nm (Figure 2). This finding strongly supports the hypothesis that the recorded spectral feature is related to the carbonation/calcination cycle and could be ascribed to some luminescence centre promoted during the thermal treatment.

Figure 2 shows the Raman spectrum of the $Ca(OH)_2$-heated samples at different temperatures (all the thermal treatments were carried out for 1 h). Besides the three vibrational modes previously reported (at 252, 357, and 680 cm^{-1}), the spectra are characterised by a large and composite contribution at 780 cm^{-1} and two new smaller peaks at 283 and 1087 cm^{-1}. In order to evidence the dependence of the 780 cm^{-1} band on the temperature, the spectra were normalised to the calcium hydroxide contribution at 357 cm^{-1} (for this reason the $Ca(OH)_2$ bands appear as faint contributions in the figure). The intensity of the 780 cm^{-1} band increases as the temperature increases up to 300 °C; then, it largely decreases, as reported in the inset of the figure. At the final investigated temperature (500 °C), the relative contribution of the two new bands at 283 and 1087 cm^{-1} increases, showing the formation of calcite (external E_g and internal A_{1g} modes, respectively) [4,33].

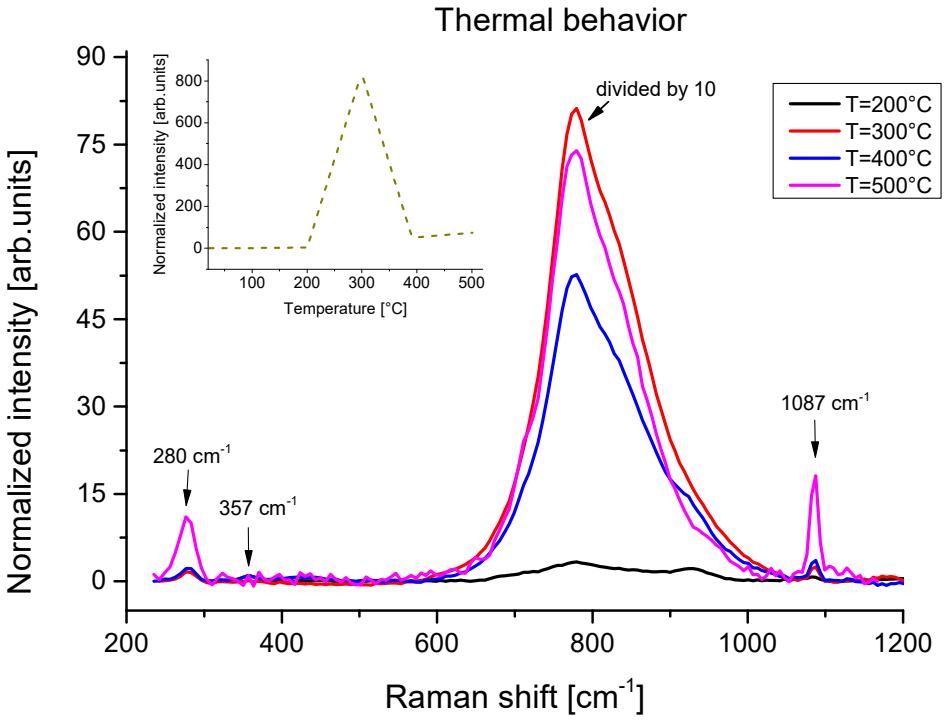

Figure 2. Raman spectra with 1064 source of lime paste heated at different temperatures for 1 h in the air (the curve at 300 °C was arbitrarily divided by 10 for clarity purposes). The insert shows the normalised intensity of the bands at 1170 nm for the different temperatures.

The observation of the two calcite bands suggests that the carbonation process is ignited by the thermal treatment. In order to understand the possible connection between the formation of the 780 cm^{-1} luminescence band and the carbonation process, we carried out the thermal treatment at 300 °C (corresponding to the maximum recorded for the 780 cm^{-1} intensity) under different environments, namely in air and under nitrogen flux. The latter was exploited to eliminate the presence of other possible reactive gasses, such as CO_2 and O_2 present in air. The Raman spectra of lime paste heated in air and in nitrogen at 300 °C and excited at 523 and 1064 nm are reported in Figure 3. The intensities are arbitrarily normalised to the peak of calcium hydroxide at 357 cm^{-1}.

Confirming the previous results, the 780 cm^{-1} band can only be detected under 1064 nm excitation, whilst no contribution is recorded under visible excitation. The spectra clearly indicate that the 780 cm^{-1} luminescence band is largely decreased when the thermal treatment is performed in nitrogen flux. We estimated the relative contribution of the 780 cm^{-1} band with respect to the calcium hydroxide 357 cm^{-1} band, the ratio increasing from 0.83 in nitrogen-treated samples up to 27 in the sample treated in the air.

As for the presence of calcite, we estimated its contribution by measuring the ratio of the 1087 cm^{-1} band with respect to the 357 cm^{-1} band. The calcite relative content is larger in the sample treated in the air (the ratio is 0.87) than in the sample treated in nitrogen (0.23).

Based on these results, two considerations can be deduced: first, the carbonization process is faster in oxidizing atmosphere; second, we found a confirmation that the band is indeed a luminescence one, and, in addition, we propose to assign it to some defect of the crystal structure possibly interacting with the O_2 molecule or promoted by the interaction/reaction with it.

To further characterise the kinetics of the formation of the 780 cm^{-1} luminescence band, we investigated its temporal evolution by monitoring the Raman spectrum excited at 1064 nm for several days. The analysis was carried out on the samples treated at different temperatures by leaving them in the air at room temperature and under standard RH conditions (60%). Figure 4 shows the spectra for the samples heated to 90 °C and arbitrarily normalised to the 1087 cm^{-1} calcite peak. In the

luminescence region, no emission bands are detected, whilst the peak of calcium hydroxide (357 cm^{-1}) decreases during the time, suggesting that the carbonation of lime paste takes place.

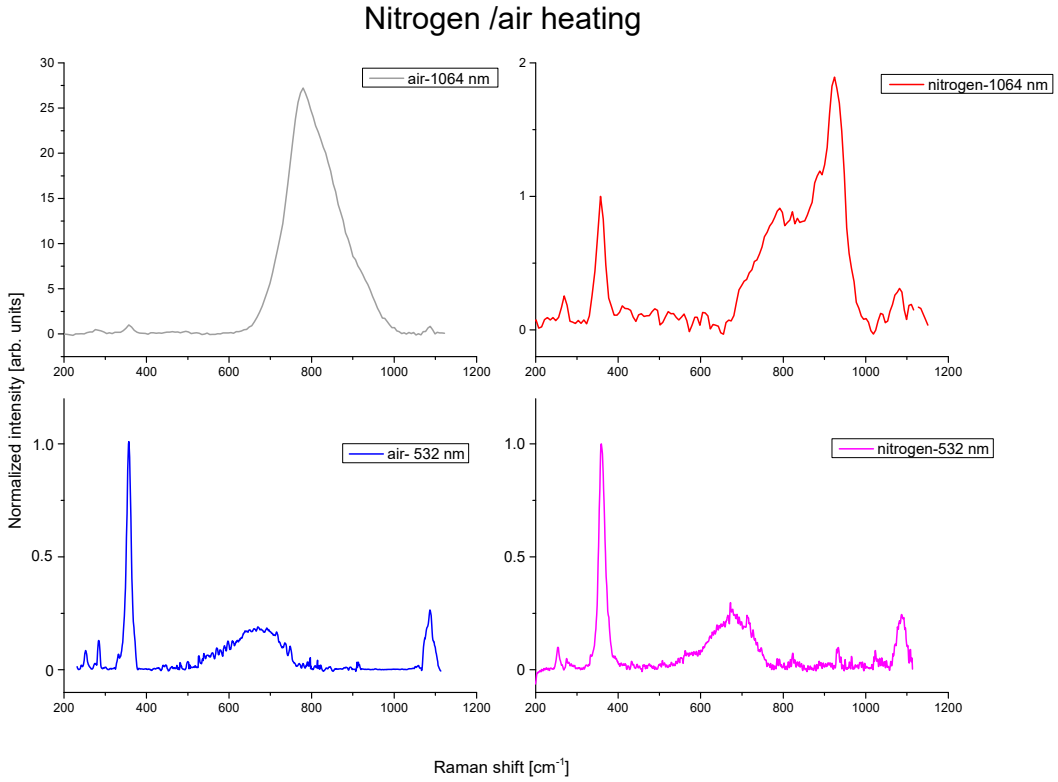

Figure 3. Raman spectra of paste lime heated in air and in N_2 atmosphere for 1 h at 300 °C with 532 and 1064 nm.

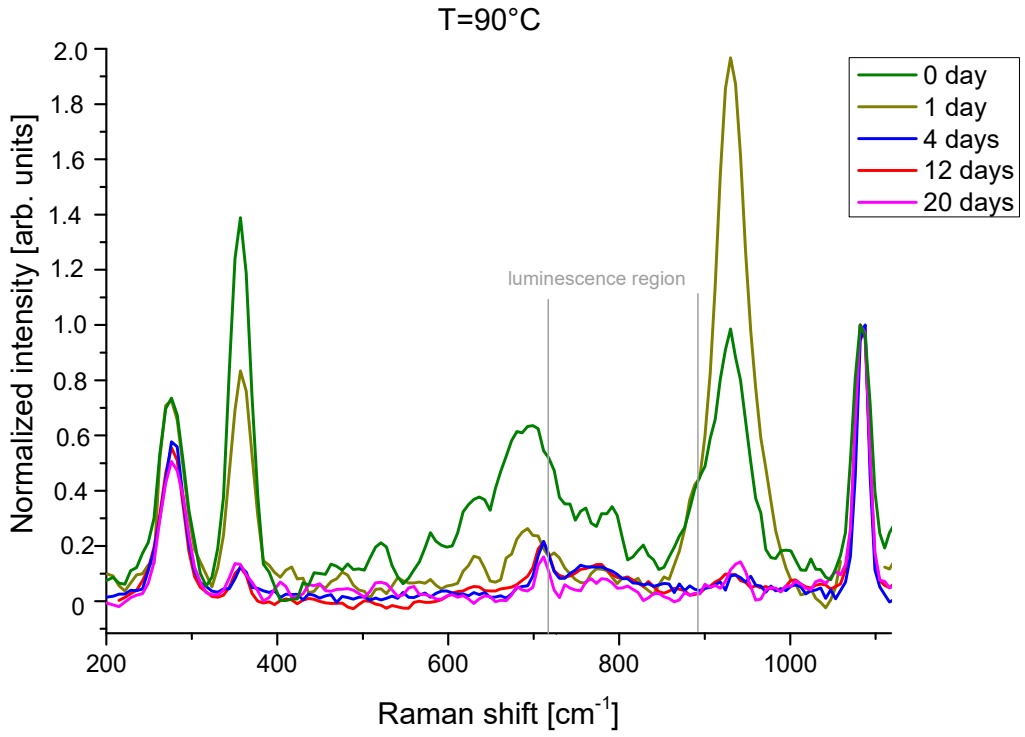

Figure 4. Dependence of the luminescence bands with the time of heated samples at T = 90°.

Indeed, in the time zero spectrum we observe both the contribution of the peak around 936 cm^{-1} attributed to the O–H out-of-plane band [31,32,34] and the one of calcium hydroxide at 357 cm^{-1}, the former being higher than the latter; then, after four days both features strongly decreased, indicating that the free water and the calcium hydroxide reacted to form calcite.

The Raman spectra of the sample heated to 200–500 °C are reported in Figure 5. In general, the luminescence band at 780 cm^{-1} is observed for all the temperatures at the time zero spectrum and it undergoes a large decrease as a function of time (see inset). The contribution of free water is clearly singled out only in the time zero spectrum of the sample treated at 200 °C spectra, whilst in the other cases no free water contribution is detected, suggesting that, as expected, at a higher temperature the whole nested water is eliminated by the thermal treatment. The whole set of samples displays the formation of calcite in the first days of observation.

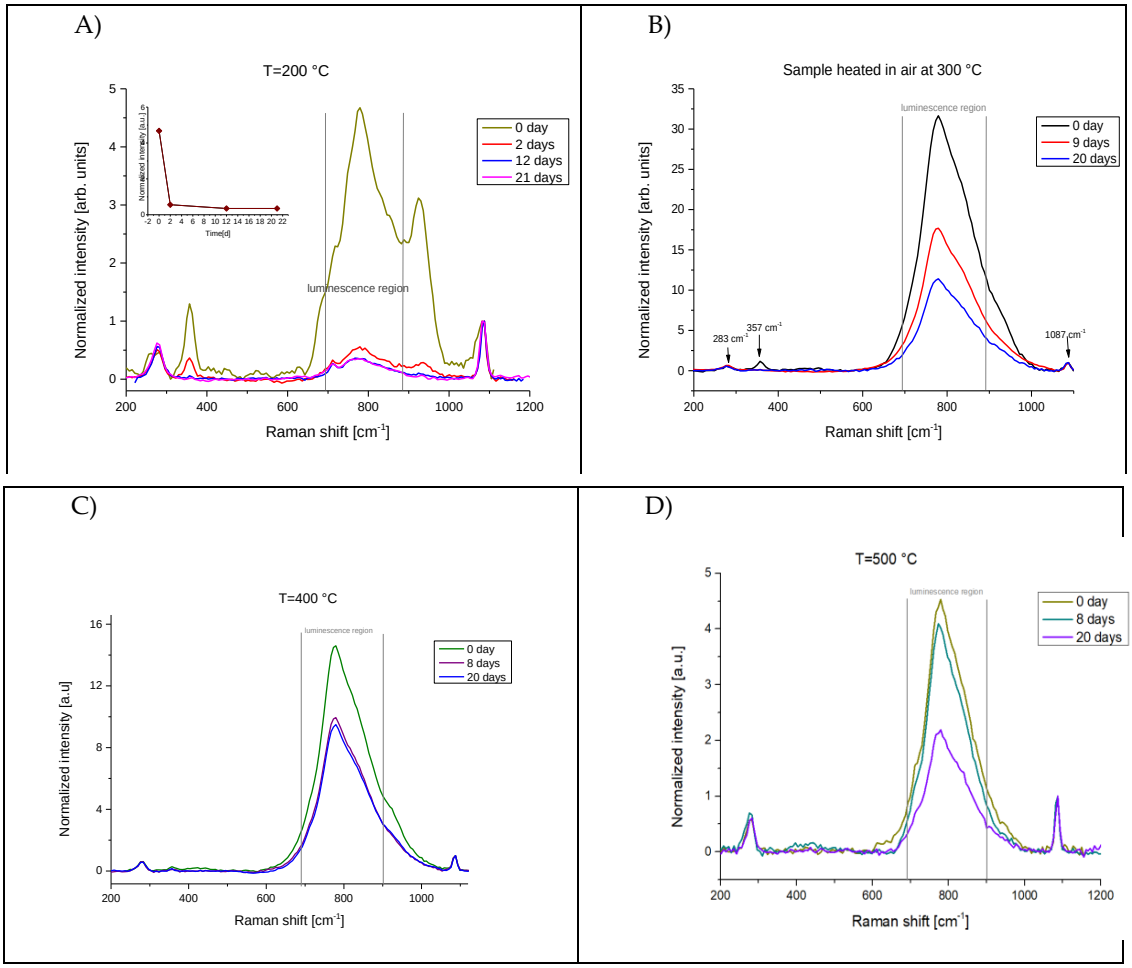

Figure 5. Dependence of the luminescence bands with the time of samples heated in air at T = 200 °C (**A**), 300 °C (**B**), 400 °C (**C**), and 500 °C (**D**).

Finally, we performed the same analysis on the samples treated under nitrogen flux (Figure 6). Besides the smaller contribution of the 780 cm^{-1} luminescence band already noted in the time zero spectrum, we also observed that the band undergoes a larger relative decrease than in air, its relative intensity being reduced by a factor of 6 in nine days for the nitrogen-treated sample, as compared to a reduction of a factor of 2 in the same observation time for the air-treated sample.

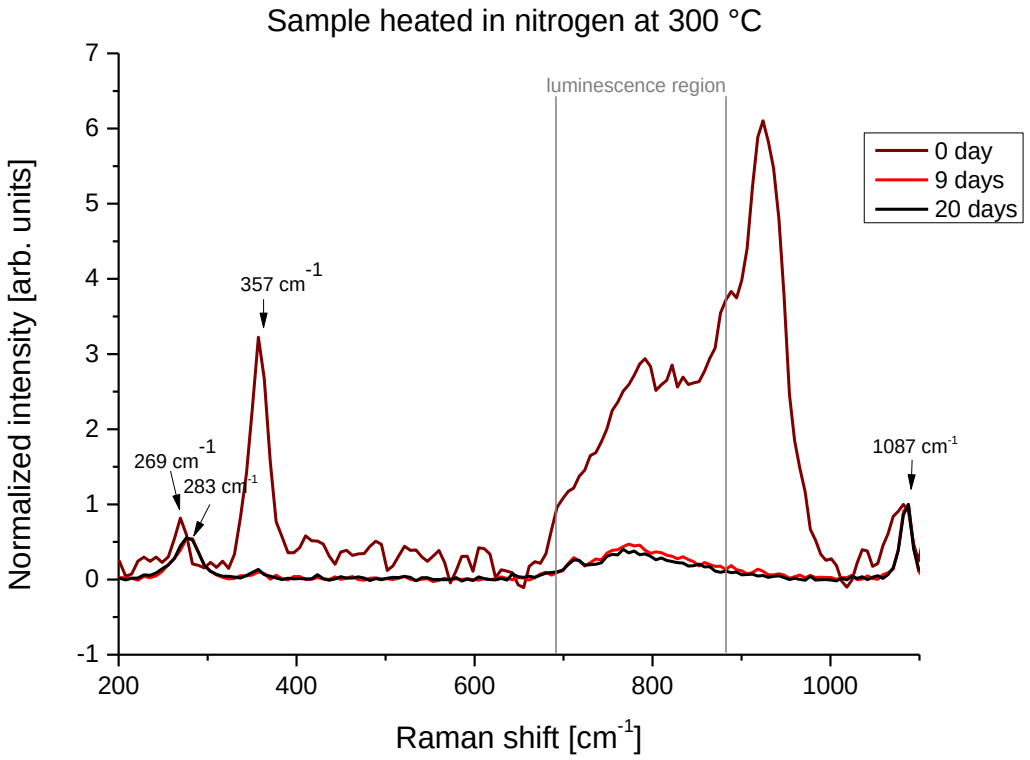

Figure 6. Dependence of the luminescence bands with the time of nitrogen-heated samples at T = 300 °C.

According to these findings, we can hypothesise a kinetic model of the carbonation process that can be monitored from the relative intensities of the Raman band at 1087 cm^{-1} (calcite) and the luminescence band at 780 cm^{-1} that we tentatively assigned to some calcium hydroxide crystal defect interacting with molecular oxygen [35,36]. The formation of calcite is somehow related to the decrease of the 780 cm^{-1} luminescence band, suggesting that the defect responsible for that luminescence is involved in the carbonation process. One can hypothesise that the defect centre is largely reactive to environment CO_2, thus acting as a seed for the carbonation process. To monitor the kinetic of the reaction, we consider the relative contribution of defects centres (counted by the intensity of the 780 cm^{-1} luminescence band) and the already formed calcite crystals (counted by the 1087 cm^{-1} Raman band). We express the starting ratio as $\boldsymbol{R_0} = \frac{I_{780}}{I_{1087}}$. When the time increases, the carbonation process occurs, and the luminescence band decreases. To evaluate the fraction of emitting centres undergoing carbonation at time $\boldsymbol{t}$ with respect to the starting population, we calculate the normalised ratio $\boldsymbol{R_n}$ defined as follows:

$$\boldsymbol{R_n(t)} = \frac{\boldsymbol{R_t}}{\boldsymbol{R_0}} = \frac{\frac{I_{780}}{I_{1087}}(\boldsymbol{t})}{\frac{I_{780}}{I_{1087}}(\boldsymbol{0})}, \quad (4)$$

where the term $\frac{I_{780}}{I_{1087}}(\boldsymbol{0})$ represents the relative starting concentration of emitting defective centres with respect to the amount of calcite crystals after the thermal treatment, and $\frac{I_{780}}{I_{1087}}(\boldsymbol{t})$ indicates the relative concentration of the defects at the instant $\boldsymbol{t}$ during the progressive carbonation process. By assuming a first order kinetic, in agreement with the model proposed by Camerini et al. in [37], a rate equation can be found, as follows:

$$\alpha = \gamma[1 - \mathrm{R_n(t)}] = \gamma(1 - \mathrm{e}^{-\frac{t}{\tau}}), \quad (5)$$

where α is the carbonation degree, τ represents the characteristic time of the process, and γ is the maximum carbonation relative value (asymptotic value in the graph).

Figure 7 reports the calculated model from experimental data recorded over 90 days for the whole set of samples, that is the ones treated at different temperatures and under different environments. The

first order kinetic model successfully fits the acquired data but for the 500 °C treated sample, where a second-order kinetics is observed, suggesting that a second carbonation process is occurring beside the previously described one. It is important to underline that the first-order kinetic model accounts for the fraction of centres that can be transformed into calcite, the final amount being dependent on the thermal treatment undergone by the sample. The curves show that the process is slower for the samples treated at 90 °C (τ = 10 days), and is the fastest at 200 °C, where the luminescence band had its maximum of intensity at zero time (τ = 0.7 days); then, it decreases its speed down to τ = 25 days for the 400 °C samples. Finally, at 500 °C the kinetics changes, as explained before. We can also note that the nitrogen-treated samples (at 300 °C) had a trend comparable with the 200 °C samples (in air) with a slightly smaller final relative value of the carbonated centres.

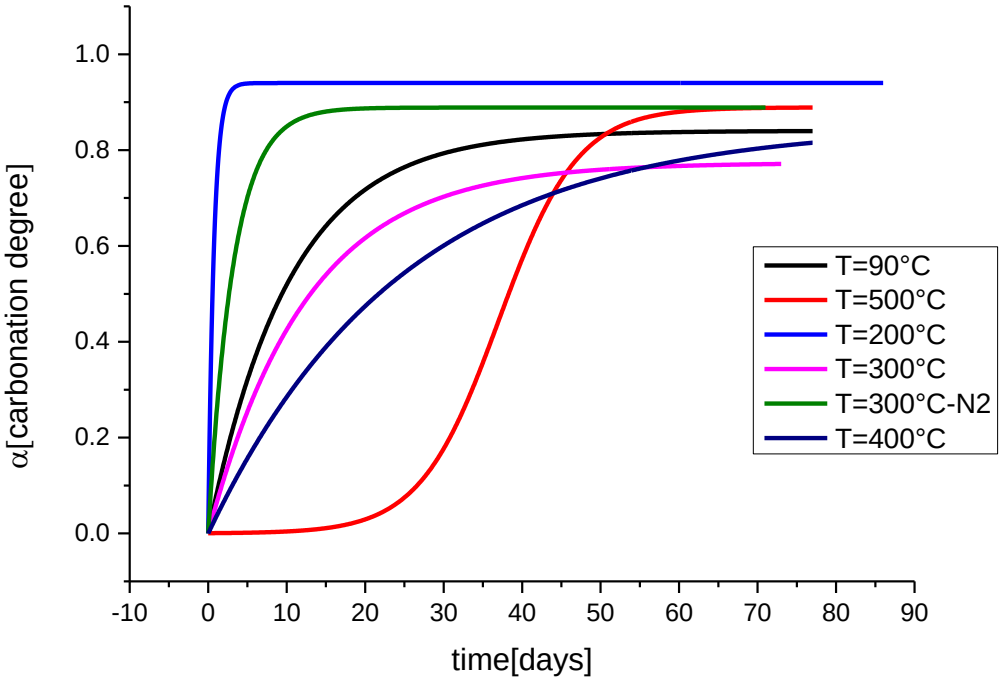

Figure 7. Kinetic model of our experimental data using Equation (2).

4. Conclusions

In this study, we carried out a detailed optical analysis (photoluminescence excitation measurements in the 200–500 nm spectral range and Raman measurements with laser sources at 405 nm, 532 nm, 632.8, and 1064 nm) of lime paste to definitively assign the nature of the band located at about 1160 nm (780 cm^{-1} under 1064 nm excitation). The 780 cm^{-1} band is present in mural paintings, in ancient mortars, and in plasters, and a complete understanding of its nature can be useful in the field of Cultural Heritage. In addition, it is also observed in modern synthetic lime paste, applied in the dentistry branch or to the construction industry.

Thermal treatments of the samples at different temperatures in the 90–500 °C range reveal different optical features and time trends. Only the Raman spectra realised with excitation of 1064 nm revealed the presence of this strong band when the sample was heated at 200 °C or above, supporting the hypothesis of a luminescent centre. The intensity of the band is related to the heating process temperature, showing a maximum at 300 °C. By changing the environment from a reducing to an oxidizing one, we evidenced that the interaction with molecular oxygen, and possibly carbon dioxide, is required to produce the defective centre. Finally, the centre acts as a preferential site for the carbonation process of the powders observed during the aging of the samples over 90 days, as indicated by the monomolecular model successfully applied to samples treated below 500 °C. The thermal treatments carried out clearly reveal that the carbonation cycle is involved in the formation of the 780 cm^{-1} band,

evidencing a correlation between the latter and the temperature, with a maximum at 300 °C. Thus, by exciting a specific artifact or a lime paste at 1064 nm and recording the luminescence/Raman spectrum, one can infer, from the relative contribution of the detected features, the history of the sample and exploit the recorded kinetic curves to develop a dating model of Cultural Heritage relics, such as "a fresco" paintings.

Author Contributions: Conceptualization, D.C. and F.A.P.; methodology, F.A.P., P.C.R.; validation, D.C.; formal analysis, F.A.P.; investigation, F.A.P.; data curation, F.A.P.; writing—original draft preparation, F.A.P.; writing—review and editing, C.M.C.; supervision, D.C., C.M.C. All authors have read and agreed to the published version of the manuscript.

Funding: This research received no external funding.

Acknowledgments: The authors thank the Reviewers and the Editors for all comments and suggestions, which helped them to improve the quality of the article.

Conflicts of Interest: The authors declare no conflict of interest.

References

1. Stojanovic, B.D.; Dzunuzovic, A.S.; Ilic, N.I. Review of methods for the preparation of magnetic metal oxides. In *Magnetic, Ferroelectric, and Multiferroic Metal Oxides*; Elsevier: Amsterdam, The Netherlands, 2018; pp. 333–359.
2. Doble, M.; Kruthiventi, A.K. Industrial Examples. In *Green Chemistry and Engineering*; ACS Publications: Washington, DC, USA, 2007.
3. Zakaria, M.N.; Sidiqa, A.N.; Artilia, I.; Cahyanto, A. Synthesis and characterization of calcium hydroxide from Indonesian limestone as endodontic intracanal medicament. In *Key Engineering Materials*; Trans Tech Publications Ltd.: Stafa-Zurich, Switzerland, 2018; Volume 782, pp. 268–272.
4. Sang, H.C.; Jin, K.P.; Seung, K.L.; Sung, M.J.; Im, H.K.; Ji, W.A.; Hwan, K. Synthesis of precipitated calcium carbonate using a limestone and its application in paper filler and coating color. In *Materials Science Forum*; Trans Tech Publications Ltd.: Stafa-Zurich, Switzerland, 2007; Volume 544, pp. 881–884.
5. Chiriu, D.; Desogus, G.; Pisu, F.A.; Fiorino, D.R.; Grillo, S.M.; Ricci, P.C.; Carbonaro, C.M. Beyond the surface: Raman micro-SORS for in depth non-destructive analysis of fresco layers. *Microchem. J.* **2019**, *153*, 104404. [CrossRef]
6. Kwon, T.Y.; Fujishima, T.; Imai, Y. FT-Raman spectroscopy of calcium hydroxide medicament in root canals. *Int. Endod. J.* **2004**, *37*, 489–493. [CrossRef]
7. Böke, H.; Akkurt, S.; Ipekoğlu, B.; Uğurlu, E. Characteristics of brick used as aggregate in historic brick-lime mortars and plasters. *Cem. Concr. Res.* **2006**, *36*, 1115–1122. [CrossRef]
8. Sébaïbi, Y.; Dheilly, R.M.; Quéneudec, M. A study of the viscosity of lime-cement paste: Influence of the physico-chemical characteristics of lime. *Constr. Build. Mater.* **2004**, *18*, 653–660. [CrossRef]
9. D'Armada, P.; Hirst, E. Nano-lime for consolidation of plaster and stone. *J. Archit. Conserv.* **2012**, *18*, 63–80. [CrossRef]
10. Silva, B.A.; Ferreira Pinto, A.P.; Gomes, A. Influence of natural hydraulic lime content on the properties of aerial lime-based mortars. *Constr. Build. Mater.* **2014**, *72*, 208–218. [CrossRef]
11. Mohammadi, Z.; Shalavi, S.; Yazdizadeh, M. Antimicrobial Activity of Calcium Hydroxide in Endodontics: A Review. *Chonnam Med. J.* **2012**, *48*, 133–140. [CrossRef] [PubMed]
12. Foreman, P.C.; Barnes, I.E. A review of calcium hydroxide. *Int. Endod. J.* **1990**, *23*, 283–297. [CrossRef]
13. Dentistry, C. Endodontology Case Reports on the Clinical Use of Calcium Hydroxide Points As an Intracanal. *Endodontology* **2006**, *18*, 23–27.
14. Denninger, E. What is 'bianco di san giovanni' of cennino cennini? *Stud. Conserv.* **1974**, *19*, 185–187.
15. Kriznar, A.; Ruiz-Conde, A.; Sánchez-Soto, P.J. Microanalysis of Gothic mural paintings (15th century) in Slovenia: Investigation of the technique used by the masters. *X-Ray Spectrom.* **2008**, *37*, 360–369. [CrossRef]
16. Chiriu, D.; Ricci, P.C.; Cappellini, G. Raman characterization of XIV–XVI centuries Sardinian documents: Inks, papers and parchments. *Vib. Spectrosc.* **2017**, *92*, 70–81. [CrossRef]

17. Chiriu, D.; Ricci, P.C.; Carbonaro, C.M.; Nadali, D.; Polcaro, A.; Mocci, F. Drying oil detected in mid-third Millennium B.C. Mesopotamian clay artifacts: Raman spectroscopy and DFT simulation study. *Microchem. J.* **2016**, *124*, 386–395. [CrossRef]
18. Chiriu, D.; Ricci, P.C.; Carbonaro, C.M.; Nadali, D.; Polcaro, A.; Collins, P. Raman identification of cuneiform tablet pigments: Emphasis and colour technology in ancient Mesopotamian mid-third millennium. *Heliyon* **2017**, *3*, e00272. [CrossRef]
19. Chiriu, D.; Ricci, P.C.; Cappellini, G.; Salis, M.; Loddo, G.; Carbonaro, C.M. Ageing of ancient paper: A kinetic model of cellulose degradation from Raman spectra. *J. Raman Spectrosc.* **2018**, *49*, 1802–1811. [CrossRef]
20. Chiriu, D.; Ricci, P.C.; Scattini, M.; Polcaro, A.; D'Andrea, M.; Richard, S.; Qader, A.A.; Carbonaro, C.M. Portable NIR Raman microspectroscopy investigation on Early Bronze IV pottery (2500–1950 BCE) from Khirbat Iskandar, Jordan. *Vib. Spectrosc.* **2018**, *97*, 8–15. [CrossRef]
21. Edwards, H.G.M.; Farwell, D.W.; Rozenberg, S. Raman spectroscopic study of red pigment and fresco fragments from King Herod's Palace at Jericho. *J. Raman Spectrosc.* **1999**, *30*, 361–366. [CrossRef]
22. Schmida, T.; Dariz, P. Shedding light onto the spectra of lime: Raman and luminescence bands of CaO, $Ca(OH)_2$ and $CaCO_3$. *J. Raman Spectrosc.* **2015**, *46*, 141–146. [CrossRef]
23. Aminzadeh, A. Fluorescence bands in the FT-Raman spectra of some calcium minerals. *Spectrochim. Acta Part A Mol. Biomol. Spectrosc.* **1997**, *53*, 693–697. [CrossRef]
24. Chaix-Pluchery, O.; Niepce, J.C.; Jannot, B.; Martinez, G. Evidence of a luminescence band during the thermal transformation of calcium hydroxide. *J. Solid State Chem.* **1988**, *73*, 563–566. [CrossRef]
25. Llopis, J. Luminescence of MgO and CaO Stabilized ZrO2 Crystals. *Phys. Status Solidi* **1990**, *119*, 661–667. [CrossRef]
26. Blasse, G.; Aguilar, M. Luminescence of natural calcite ($CaCO_3$). *J. Lumin.* **1984**, *29*, 239–241. [CrossRef]
27. Wang, H.Y.; Gong, F.Z.; Zhou, L.Y.; Sun, L. Facile synthesis of $CaCO_3$ and $CaCO_3$:Eu3+ phosphors by solid state reaction at room temperature and the luminescence properties. In *Materials Science Forum*; Trans Tech Publications Ltd.: Stafa-Zurich, Switzerland, 2015; Volume 809, pp. 711–718.
28. Dubina, E.; Korat, L.; Black, L.; Strupi-Šuput, J.; Plank, J. Influence of water vapour and carbon dioxide on free lime during storage at 80 C, studied by Raman spectroscopy. *Spectrochim. Acta Part A Mol. Biomol. Spectrosc.* **2013**, *111*, 299–303. [CrossRef] [PubMed]
29. Lafuente, B.; Downs, R.T.; Yang, H.; Stone, N. The power of databases: The RRUFF project. In *Highlights in Mineralogical Crystallography*; Walter de Gruyter GmbH.: Berlin/Heidelberg, Germany, 2016; ISBN 9783110417104.
30. Chaix-Pluchery, O.; Ciosmak, D.; Niepce, J.C.; Peyrard, M. Raman study of prereactional transformations in calcium hydroxide crystals during a thermal treatment leading to dehydration. *J. Solid State Chem.* **1984**, *53*, 273–276. [CrossRef]
31. Sugama, T.; Gray, G.; Kukacka, L.E. Alkali carbonation of autoclaved polymer-cement composites in Na_2CO_3-laden water at 300 °C. *J. Mater. Sci.* **1992**, *27*, 180–190. [CrossRef]
32. Sugama, T.; Brothers, L.E.; Van De Putte, T.R. Air-foamed calcium aluminate phosphate cement for geothermal wells. *Cem. Concr. Compos.* **2005**, *27*, 758–768. [CrossRef]
33. Porto, S.P.S.; Giordmaine, J.A.; Damen, T.C. Depolarization of raman scattering in calcite. *Phys. Rev.* **1966**, *147*, 608. [CrossRef]
34. Buzgar, N.; Apopei, A.I. The Raman study of certain carbonates. *Geol. Tomul L* **2009**, *2*, 97–112.
35. Kemperl, J.; Maček, J. Precipitation of calcium carbonate from hydrated lime of variable reactivity, granulation and optical properties. *Int. J. Miner. Process.* **2009**, *93*, 84–88. [CrossRef]
36. Galmarini, S.; Bowen, P. Atomistic simulation of the adsorption of calcium and hydroxyl ions onto portlandite surfaces—Towards crystal growth mechanisms. *Cem. Concr. Res.* **2016**, *81*, 16–23. [CrossRef]
37. Camerini, R.; Poggi, G.; Chelazzi, D.; Ridi, F.; Giorgi, R.; Baglioni, P. The carbonation kinetics of calcium hydroxide nanoparticles: A Boundary Nucleation and Growth description. *J. Colloid Interface Sci.* **2019**, *547*, 370–381. [CrossRef] [PubMed]